Electronic Supplementary Material (ESI) for Polymer Chemistry.

New horizons for carbon dots: nano-photoinitiating catalysts for cationic photopolymerization and three-dimensional (3D) printing under visible light

Wiktoria Tomal,[1] Tomasz Świergosz,[2] Maciej Pilch,[1] Wiktor Kasprzyk,[1] Joanna Ortyl[1,3*]

[1] Department of Biotechnology and Physical Chemistry, Faculty of Chemical Engineering and Technology, Cracow University of Technology, Warszawska 24 , 31-155 Kraków, Poland

[2] Department of Analytical Chemistry, Faculty of Chemical Engineering and Technology, Cracow University of Technology, Warszawska 24, 31-155 Kraków, Poland

[3] Photo HiTech Ltd., Bobrzyńskiego 14, 30-348 Cracow, Poland

Corresponding Author:

* Joanna Ortyl; e-mail: jortyl@pk.edu.pl

SUPPORTING INFORMATION

C O N T E N T S

Figure S18. (a) Fluorescence quenching study of N,S-co-doped-CA-CDs (0.01 mg /mL-1) in water with different adding amount of IOD; (b) Plots of ratio I_0/I versus added amount of IOD. I_0 and I represent the emission intensity in the absence and presence of IOD, respectively.

Figure S19. Excitation and emission spectra for the determination of the excited singlet state energy for N,S-co-doped-CA-CDs in water.

Figure S20. Scheme of cyclic voltammetry apparatus to investigate electrochemical properties of carbon dots (M161 Electrochemical Analyzer, Poland).

Figure S21. (a) Cyclic voltametric profiles and (b) first derivative of voltametric profiles recorded utilizing 1 mM potassium ferricyanide (Aldrich) in 0.1 M KCl, obtained using 3mm GC Disk Electrode with the addition of increasing amounts of CA-CDs.

Figure S22. (a) Cyclic voltametric profiles and (b) first derivative of voltametric profiles recorded utilizing 1 mM potassium ferricyanide (Aldrich) in 0.1 M KCl, obtained using 3mm GC Disk Electrode with the addition of increasing amounts of N-doped-C-ACDs.

Figure S23. (a) Cyclic voltametric profiles and (b) first derivative of voltametric profiles recorded utilizing 1 mM potassium ferricyanide (Aldrich) in 0.1 M KCl, obtained using 3mm GC Disk Electrode with the addition of increasing amounts of N,S-doped-CA-CDs.

Photo S1. 3D hydrogel inscription made by the free-radical photopolymerization of mixture HEA/water (1/1 wt.) in the presence of a two-component photoinitiating system based on CA-CDs (0.2 wt. %) and IOD (2 wt. %).

Figure S24. Scheme of the electron transfer mechanism proposal to generate the strong protonic acids.

Grafical abstract

Synthesis

Table S1. One-pot "bottom-up" synthesis of carbon dots.

CDs	Reagents	Reaction temperature [°C]	Reaction time [h]
CA-CDs	citric acid	230	2
N-doped-CA-CDs	citric acid/urea	230	2
N,S-doped-CA-CDs	citric acid/thiourea	230	2

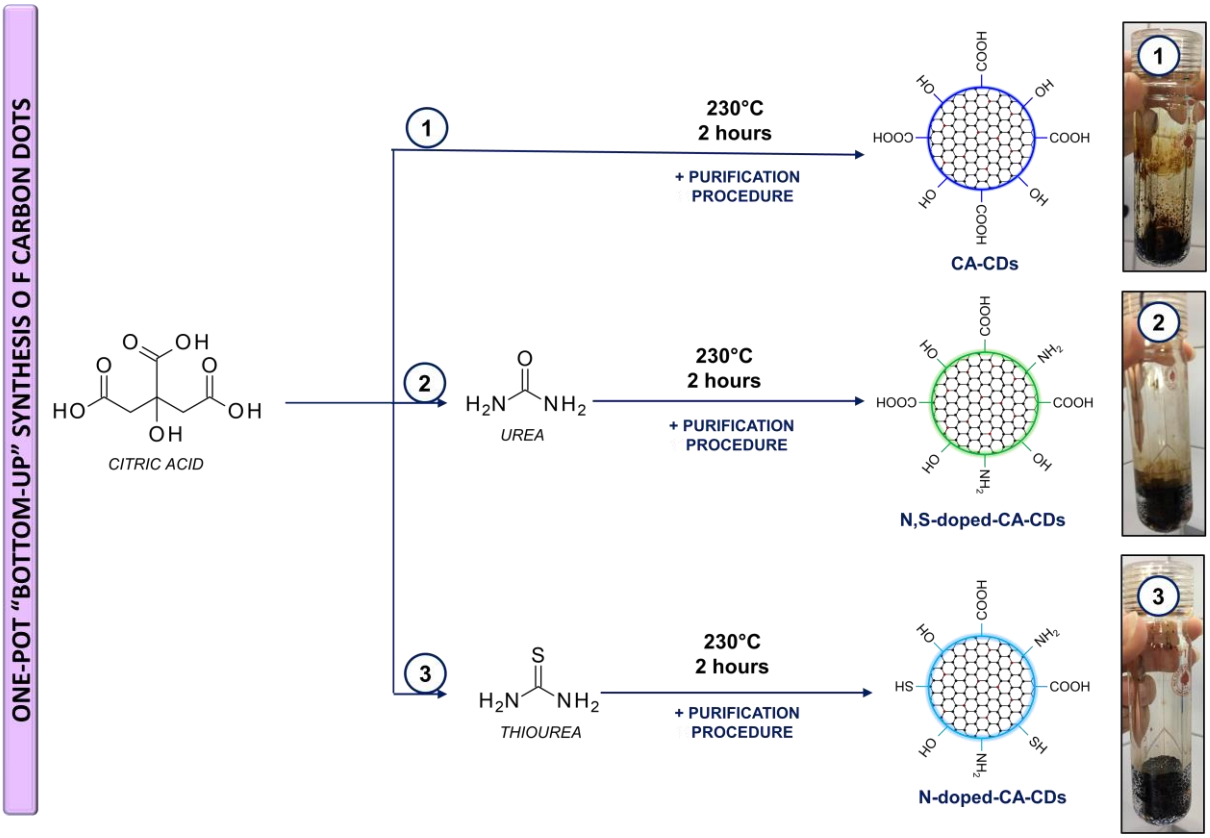

Figure S1. Scheme of one-pot "bottom-up" synthesis pathway for various carbon dots.

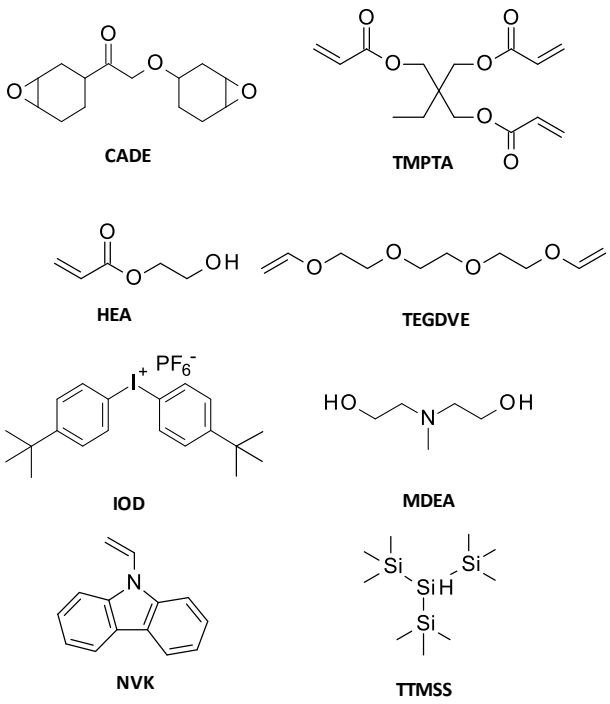

Figure S2. Structures of applied monomers and other reagents utilized in the photopolymerization processes.

Purification

Throughout the one-pot "bottom-up" hydrothermal synthesis of carbon dots, various fluorophores as by-products can be formed. In previous work (*), we introduced the results of our investigations into the elucidation of the chemical structure of moieties responsible for the blue and green luminescence of CDs derived from the microwave-assisted pyrolysis of citric acid in the presence of urea. Because during microwave as well as hydrothermal synthesis, various reaction pathways between citric acid and urea are possible. In consequence, exact analysis of the CD structure requires careful separation of the different CD fractions from the mixture. That is why we undertook to identify the molecule responsible for high QY of green fluorescence of this type materials. As a result of the work, we found that the small organic molecular fluorophore that forms during the synthesis of green fluorescing CDs is 4-hydroxy-1H-pyrrolo[3,4-c]pyridine-1,3,6-(2H,5H)-trione (HPPT). Furthermore, the above considerations lead us to the conclusion that the fabrication of carbon dots needs to be carefully separation and purification from organic compounds. Therefore, in this work, particular emphasis was placed on **properly purify the synthesized carbon dots**. The structural and optical properties of each fraction were characterized separately. In consequence the purification was carried out according to the procedure (Figure 3) and the degree of purification of carbon dots was monitored by measuring the absorbance and fluorescence of individual filtrates during the process (**Figure S4**). Finally, it was possible to separate CDs from free molecular fluorophores. The fractions that are expected to contain fluorophores show the highest fluorescence quantum yields (QY) (**Figure S5**).

* W. Kasprzyk, T. Świergosz, S. Bednarz, K. Walas, N. V. Bashmakova and D. Bogdał, Luminescence phenomena of carbon dots derived from citric acid and urea – a molecular insight, Nanoscale, 2018, 10, 13889.

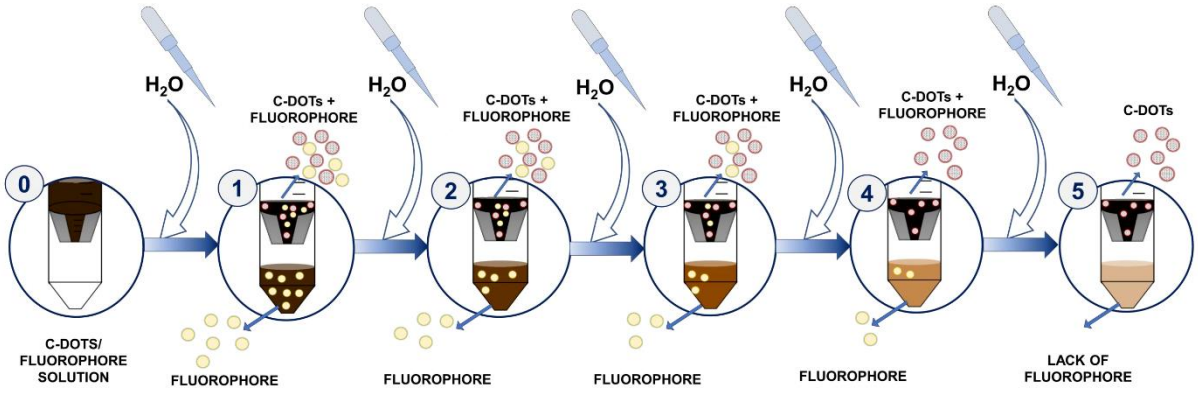

Figure S3. Scheme of carbon dot purification with the use of a centrifuge - dependence of the number of rinses on the fluorophores content in the upper layer of the falcons - layer of carbon dots.

Spectroscopic characteristics of filtrates

Each filtrate obtained during purification of carbon dots was collected into a separate Vivaspin®20 centrifugal concentrators (produced by Sartorius), and its absorbance and fluorescence were measured. The Vivaspin®20 was equipped twin vertical polyethersulfone (PES) membranes for unparalleled filtration speeds, the Vivaspin® 20 can achieve 100 x plus concentrations. As shown in Figure S3, both absorbance, and fluorescence of the filtrate decrease with each subsequent rinsing resulting in carbon dots free from the fluorophores. The crucial is the number of rinsing because it is not constant and depends on the amount of post-reaction solution mixture placed in the concentrators - the higher the concentration of carbon dots before purification is, the more times it takes to be rinsed with deionized water until the filtrate shows no fluorescence and has an absorbance close to zero.

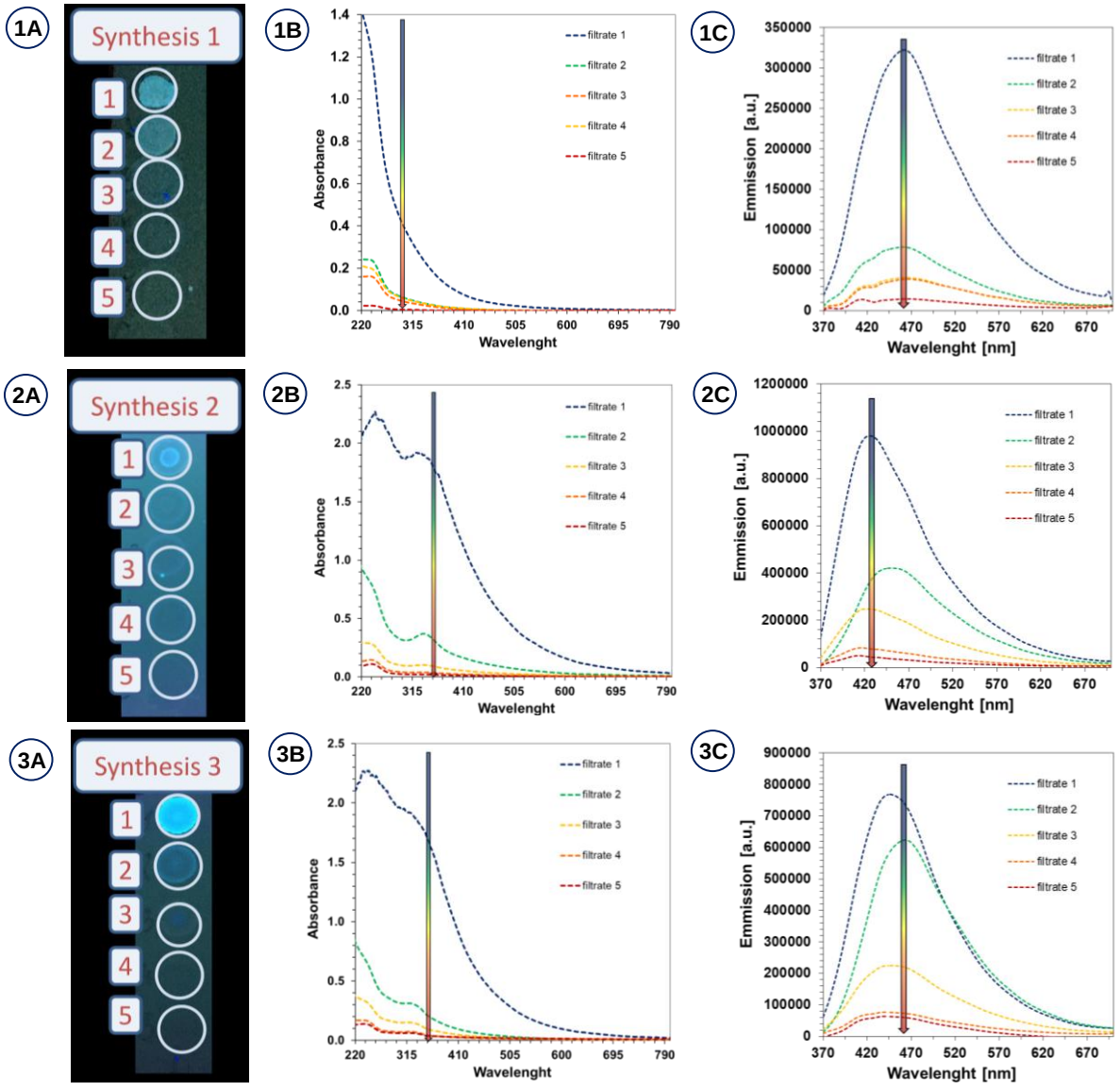

Figure S4. Spectroscopic studies on the quality of carbon dot purification procedure **1A-3A**: an obtained image of a TLC plate with the filtrate solution deposited on it; **1B-3B**: fading of absorbance as a result of washing out the fluorophore from the solution; **1C-3C**: fluorescence drop caused by washing out the fluorophore from the solution.

Spectroscopic characteristics of HPPT - small organic molecule from filtrates during purification of N-doped-CDs

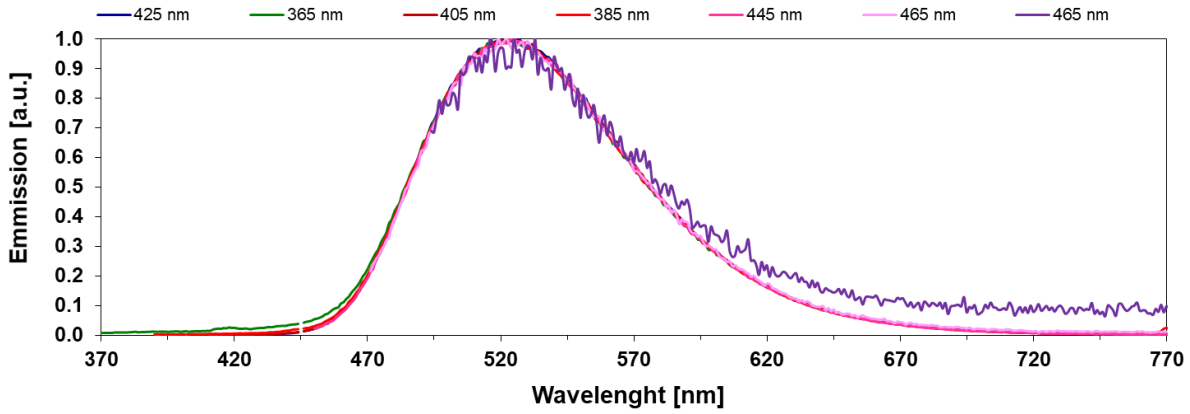

Figure S5. Fluorescent spectra of aqueous solutions of 4-hydroxy-1H-pyrrolo[3,4-c]pyridine-1,3,6-(2H,5H)-trione (HPPT) – the fluorescent small organic molecule, determined with the use of various excitation wavelengths. Normalized fluorescence emission spectra of the water solution of HPPT for comparison (the concentration of all solutions was 0.0125 mg ml^{-1}). The fluorescence spectrum of HTTP has one band with a maximum at about 540 nm.

XPS analysis

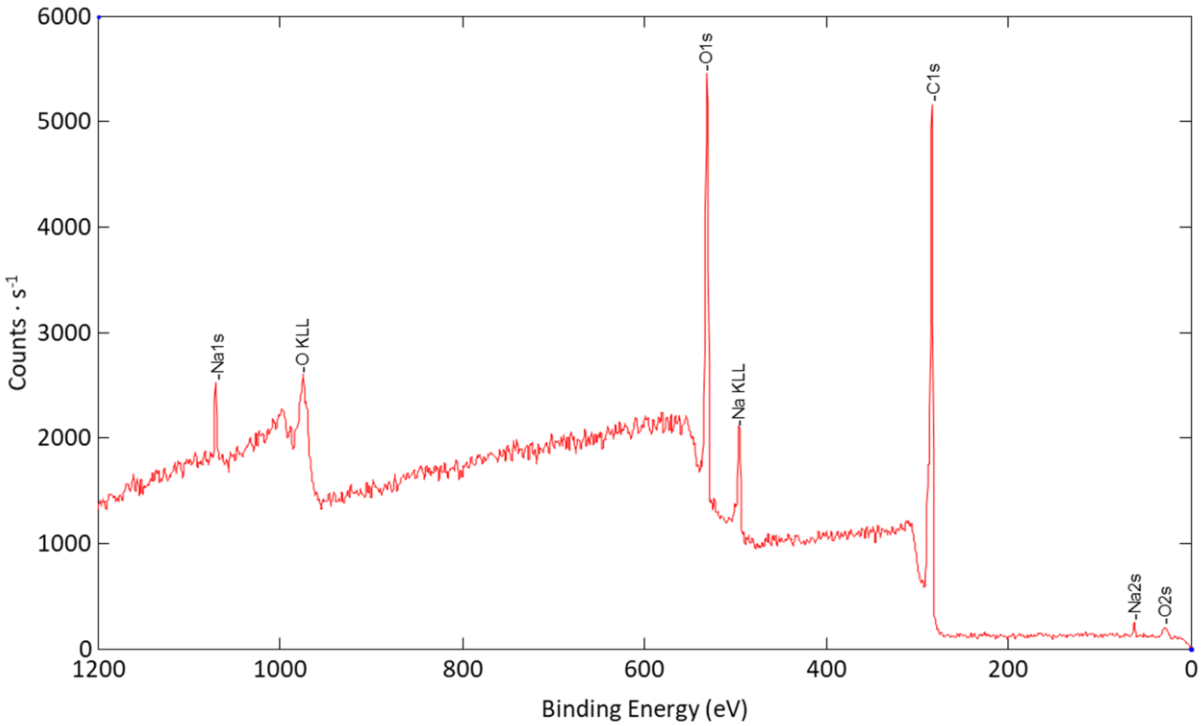

Figure S6. Survey XPS spectrum of carbon dots: CA-CDs

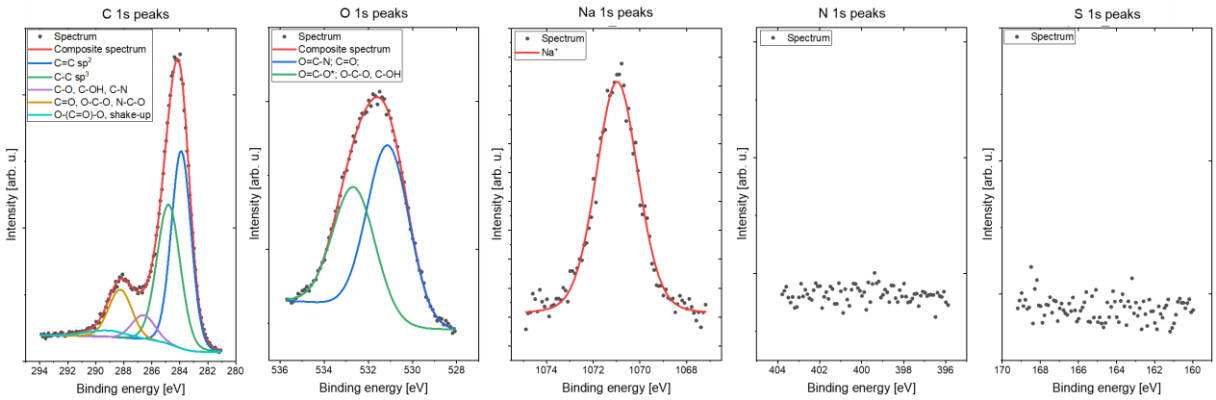

Figure S7. High resolution spectra of different peaks and analyzes for carbon dots: CA-CDs

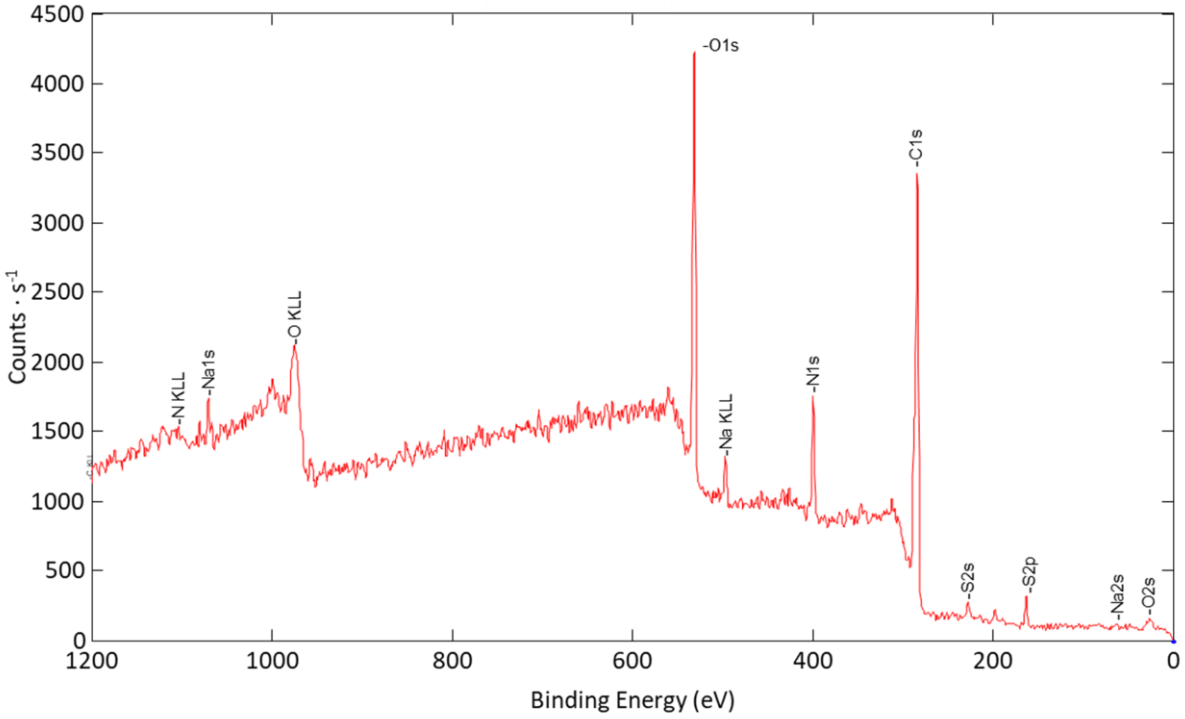

Figure S8. Survey XPS spectrum of carbon dots: N-doped-CA-CDs

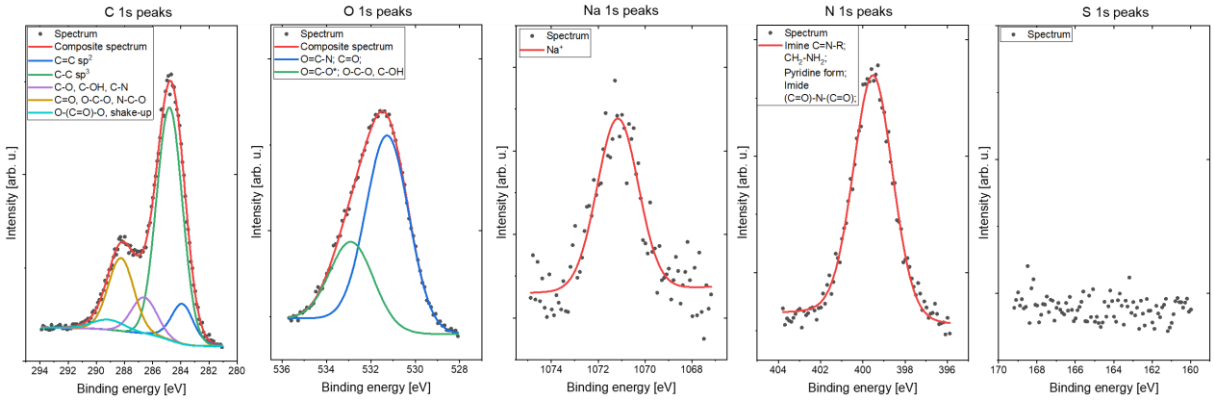

Figure S9. High resolution spectra of different peaks and analyzes for carbon dots: N-doped-CA-CDs

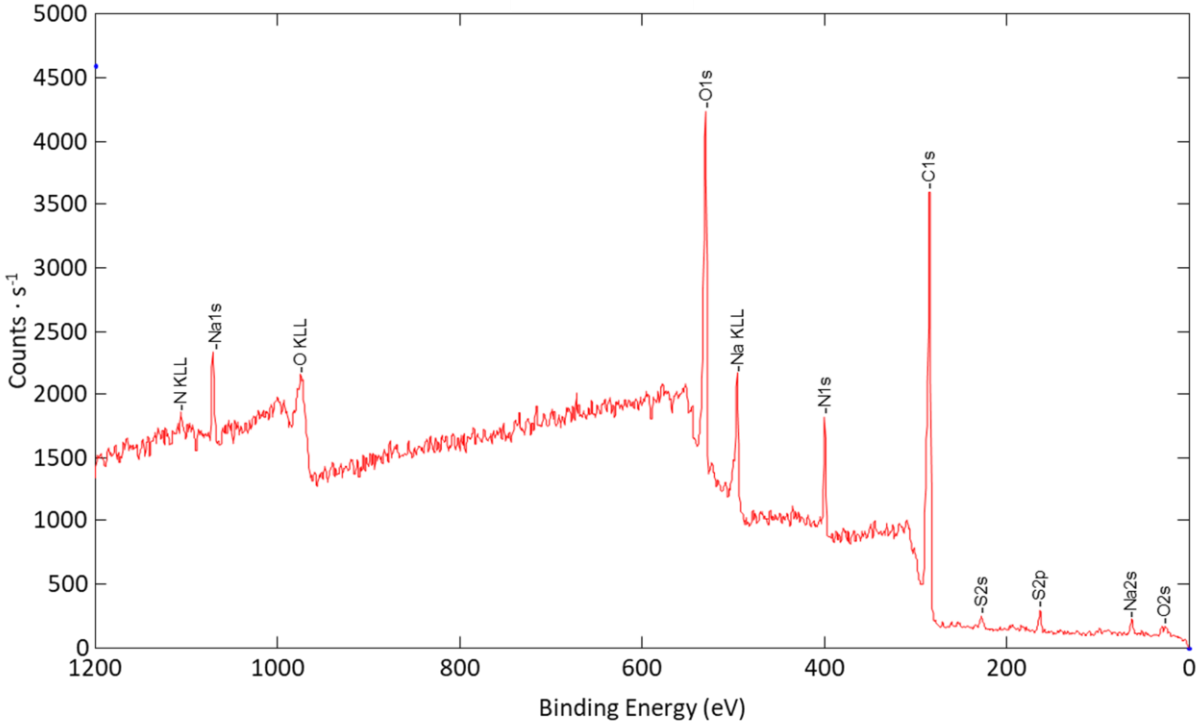

Figure S10. Survey XPS spectrum of carbon dots: N,S-doped-CA-CDs

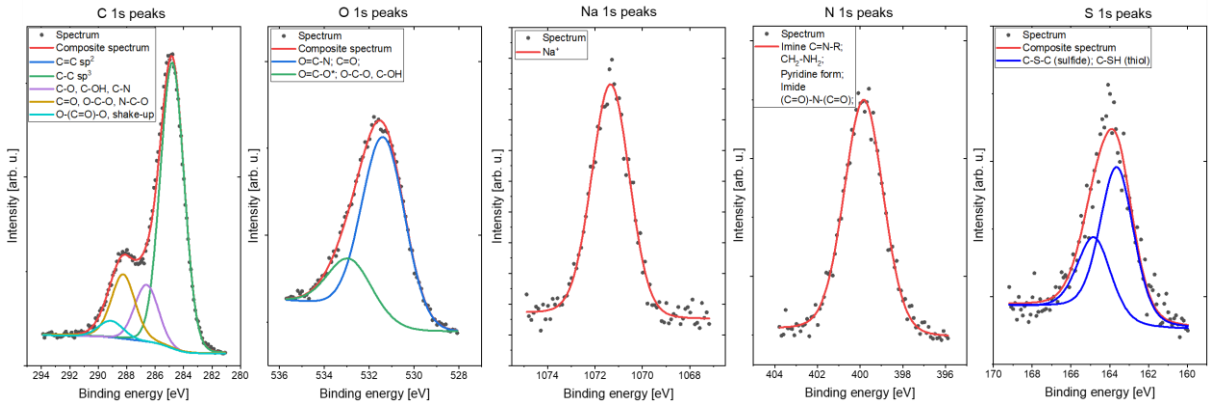

Figure S11. High resolution spectra of different peaks and analyzes for carbon dots: N,S-doped-CA-CDs

Dynamic Light Scattering (SLS) measurements

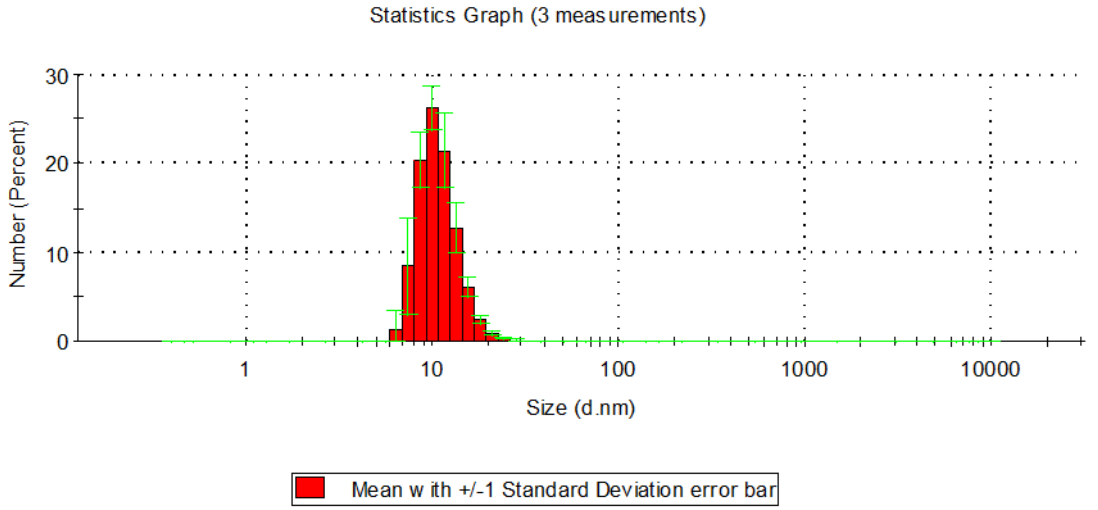

Figure S12. DLS particle size histograms of CA-CDs.

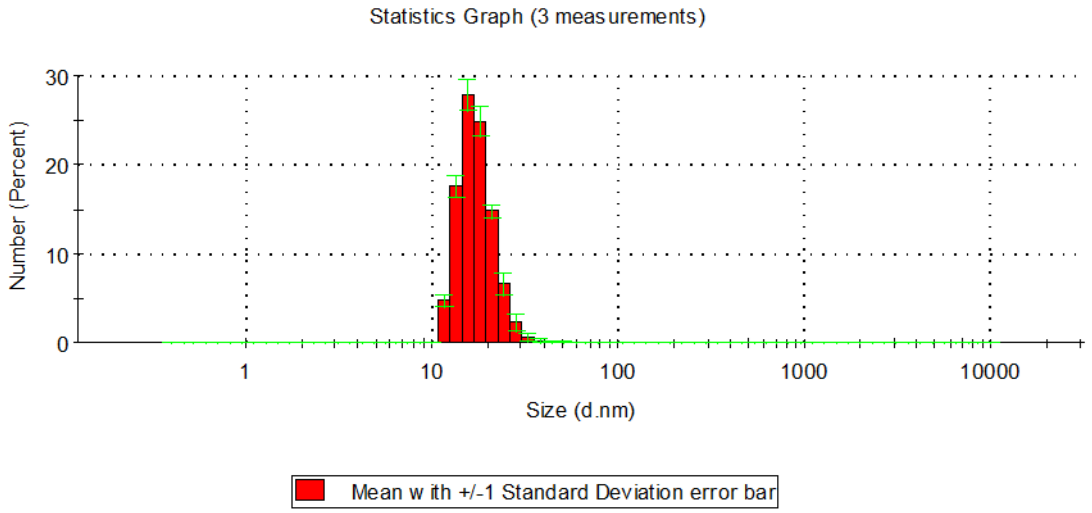

Figure S13. DLS particle size histograms of N-doped-CA-CDs.

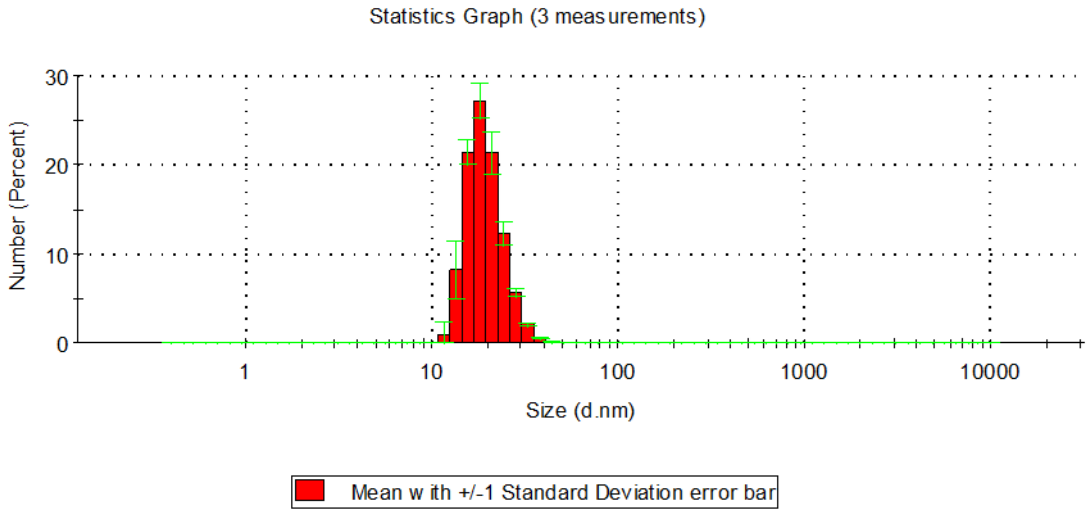

Figure S14. DLS particle size histograms of N,S-doped-CA-CDs.

Real-Time FT-IR photopolymerization experiments

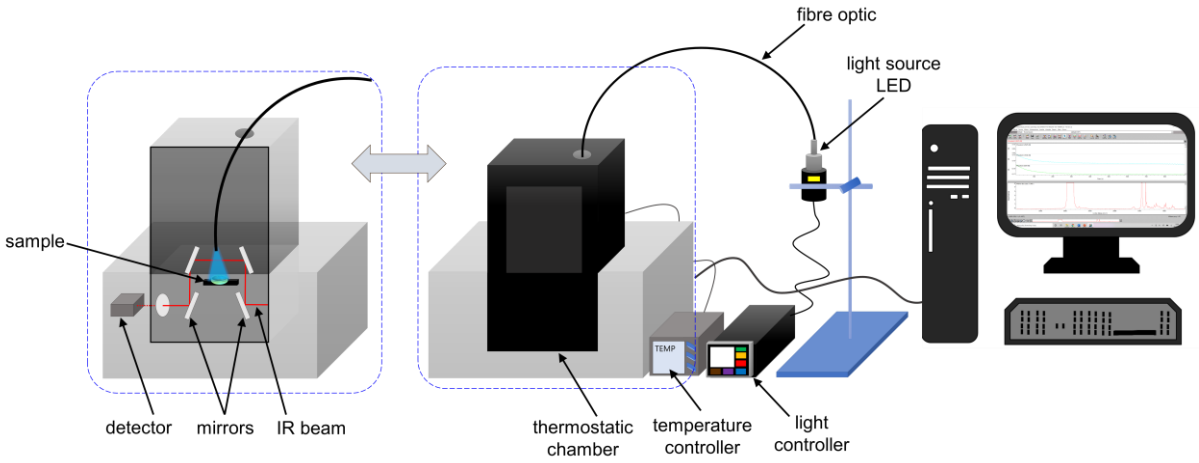

Figure S15. Scheme of Nicolet™ iS™ 10 FTIR Spectrometer (Thermo Scientific, Waltham, MA, USA) with spectral range 7800-350 cm^{-1} and with a horizontal adapter for real-time monitoring photopolymerization experiments, equipped with thermostatic chamber. Thermostatic chamber provides temperatures settable from 15°C to 36°C, provide a combination of heating and cooling producing a controlled environment with fan circulation for consistent chamber temperature. Thermostatic chamber was designed by Paweł Fiedor from Laboratory of Photochemistry and Optical Spectroscopy, Faculty of Chemical Engineering and Technology, Cracow University of Technology.

Photopolymerization processes during the preparation of hydrogel materials were carried out in the air using a specially designed attachment made of BaF_2, eliminating spectrum interference caused by the presence of water in the system. The pattern of the designed attachment is shown in **Figure S12**.

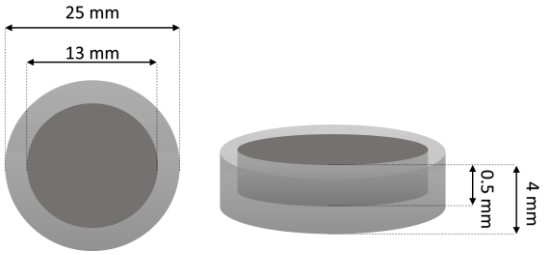

Figure S16. Barium fluoride adapter applied in the photopolymerization processes.

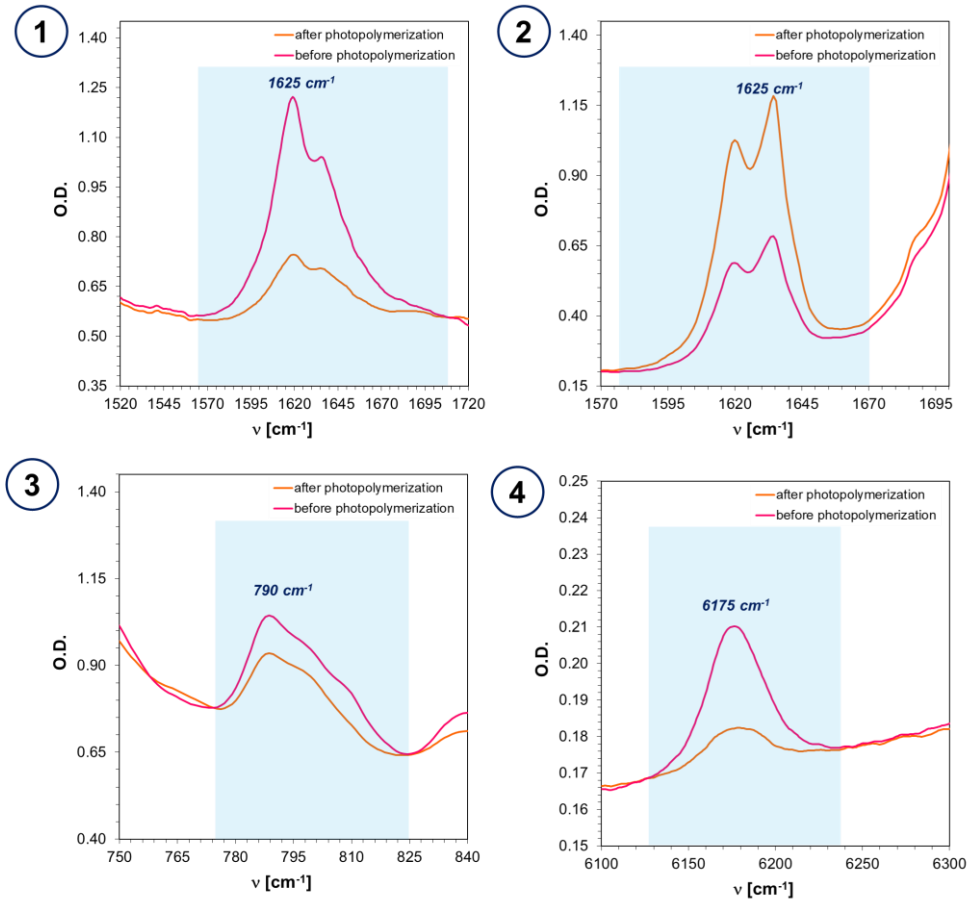

Figure S17. FT-IR spectra before and after polymerization of:
1) **TEGDVE** in the presence of CA-CDs/IOD (0.2/.0 wt. %) under LED@365 nm (thickness: 25µm);
2) **TMPTA** in the presence of CA-CDs/IOD (0.2/.0 wt. %) under LED@365 nm (thickness: 25µm);
3) **CADE** in the presence of CA-CDs/IOD (0.2/.0 wt. %) under LED@365 nm (thickness: 25µm);
4) **HEA** in the presence of CA-CDs/IOD (0.2/2.0 wt. %) under LED@365 nm (thickness: 0.5 mm).

SUPPORTING INFORMATION

Free-radical photopolymerization of acrylate monomers

Table S2. Conversions obtained for acrylate monomer during free-radical photopolymerization upon exposure UV-LED or visible LED light sources for different bimolecular photoinitiating system based on CDs.

Acronym	**Bulk photopolymerization of ACRYLATE monomer monitored at ~1,635 cm^{-1}**	
	IOD/CDs (2.0/0.2 % wt.)	
	@365nm current = 1.7A; power out = 1.15 W, irradiance = 24.8 mW/cm^2	@405nm current = 1.4A; power out = 1.50 W, irradiance = 22.0 $\mu W/mm^2$
CA-CDs	26	12
N-doped-CA-CDs	19	12
N,S-doped-CA-CDs	31	24

Photocatalytic properties of carbon dots during free-radical polymerization of the water-based coating hydrogel

Table S3. Conversions obtained for acrylate monomer during free-radical photopolymerization of hydrogel material under air condition and upon exposure visible light source LED@405nm for different photoinitiating systems.

Free-radical photopolymerization profiles of HEA/water (1:1 wt. %) mixture, monitored at ~6,125 cm^{-1}		
Composition		**Conversion [%]** @405nm current = 1.4 A; power out = 1.50 W, irradiance = 22.0 cW/cm^2
Photocurable CD-s compositions	CDs (0.2%) + IOD (2%)	40
	CDs (0.2%) + MDEA (2%)	15
	CDs (0.2%) + IOD (2%) + MDEA (2%)	98
References	IOD (2%)	24
	MDEA (2%)	4
	IOD (2%) + MDEA (2%)	14

Fluorescence quenching with iodonium salt (IOD) of investigated N,S-co-doped-CA-CDs together with Stern-Volmer correlation

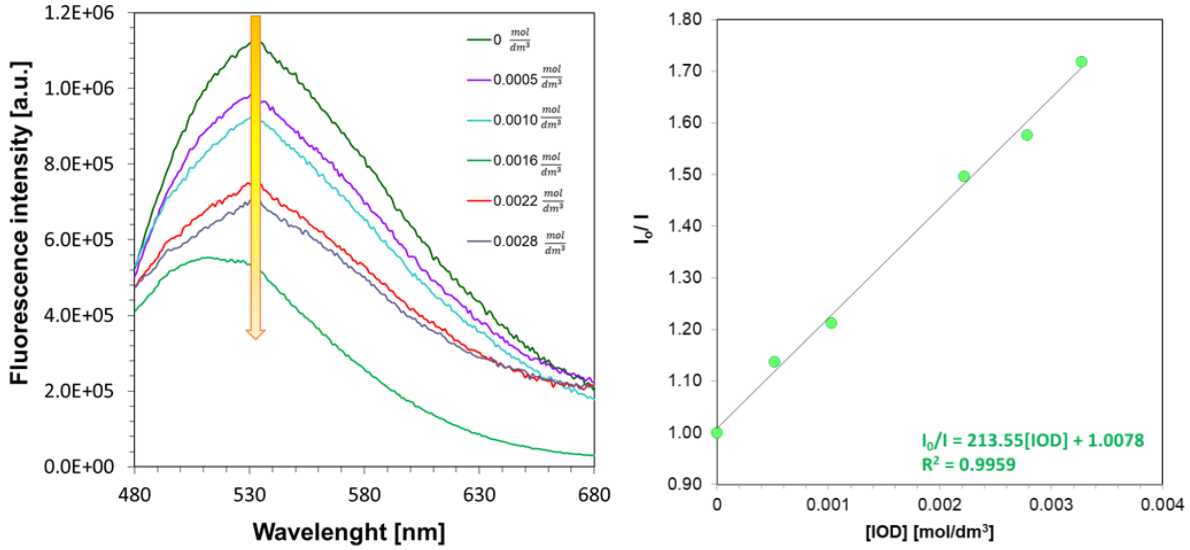

Figure S18. (a) Fluorescence quenching study of N,S-co-doped-CA-CDs (0.01 mg /mL-1) in water with different adding amount of IOD; (b) Plots of ratio I_0/I versus added amount of IOD. I_0 and I represent the emission intensity in the absence and presence of IOD, respectively.

Absorption and fluorescence spectra for the determination of the excited singlet state energy for investigated of N,S-co-doped-CA-CDs in water

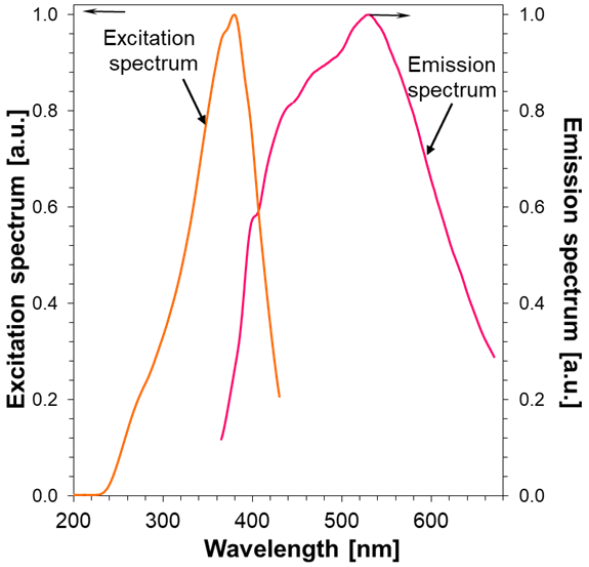

Figure S19. Excitation and emission spectra for the determination of the excited singlet state energy for N,S-co-doped-CA-CDs in water.

Cyclic voltammetry curves showing oxidation and reduction processes of CDs in water

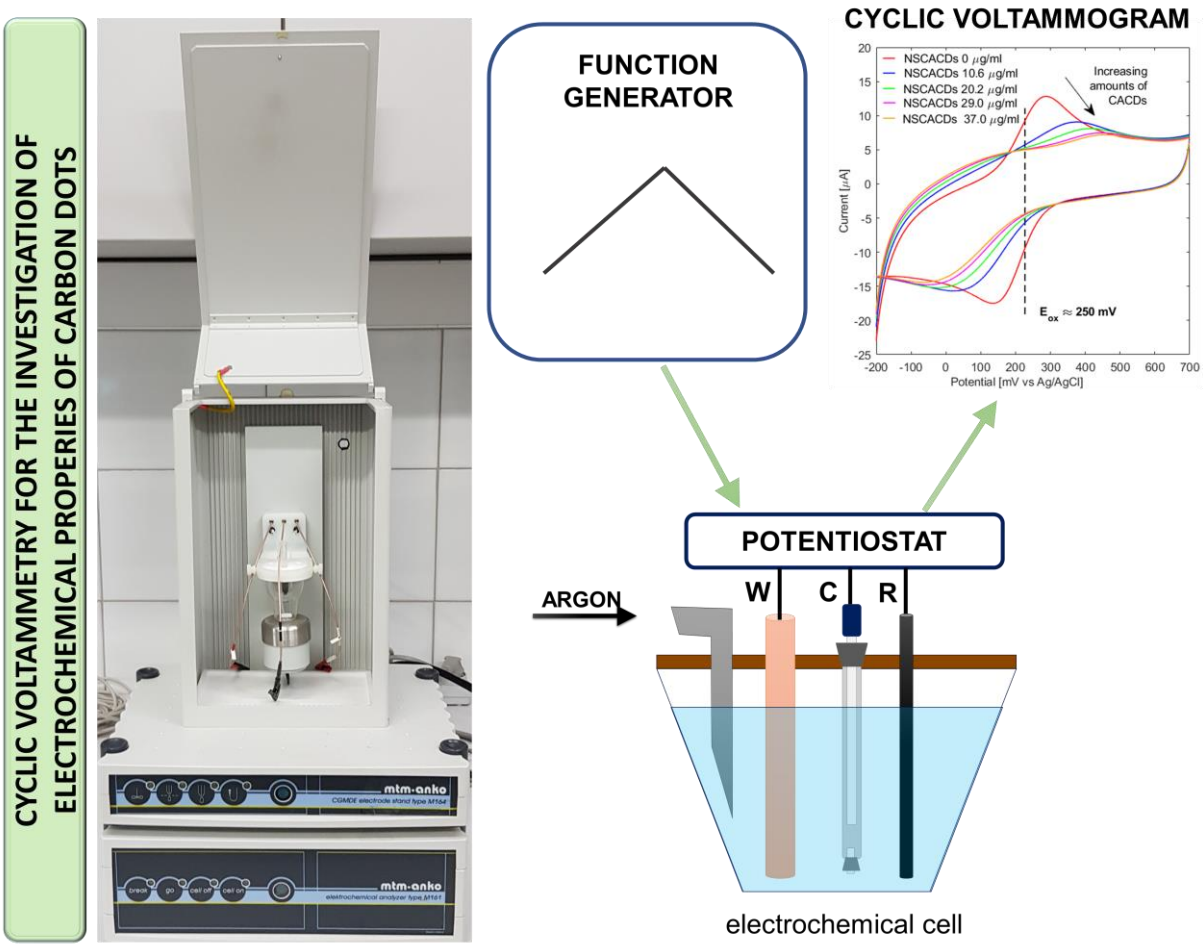

Figure S20. Scheme of cyclic voltammetry apparatus to investigate electrochemical properties of carbon dots (Electrochemical Analyzer M161 and the Electrode Stand M164, from MTM-ANKO, Poland). An argon purge was be used if desired to expel excess oxygen from the solution before measuring the current.

The typical three-electrode cell configuration used for the electrochemical measurements are:

W - the working electrode was a glassy carbon electrode of 3 mm diameter (Mineral, Poland);

R - the platinum wire acted as an auxiliary electrode;

C - all potentials were measured against the Ag/AgCl (3M KCl) electrode, which was placed in a double bridge, filled with 3M KCl solution in the upper part and a supporting electrolyte solution in a given solvent in the lower part.

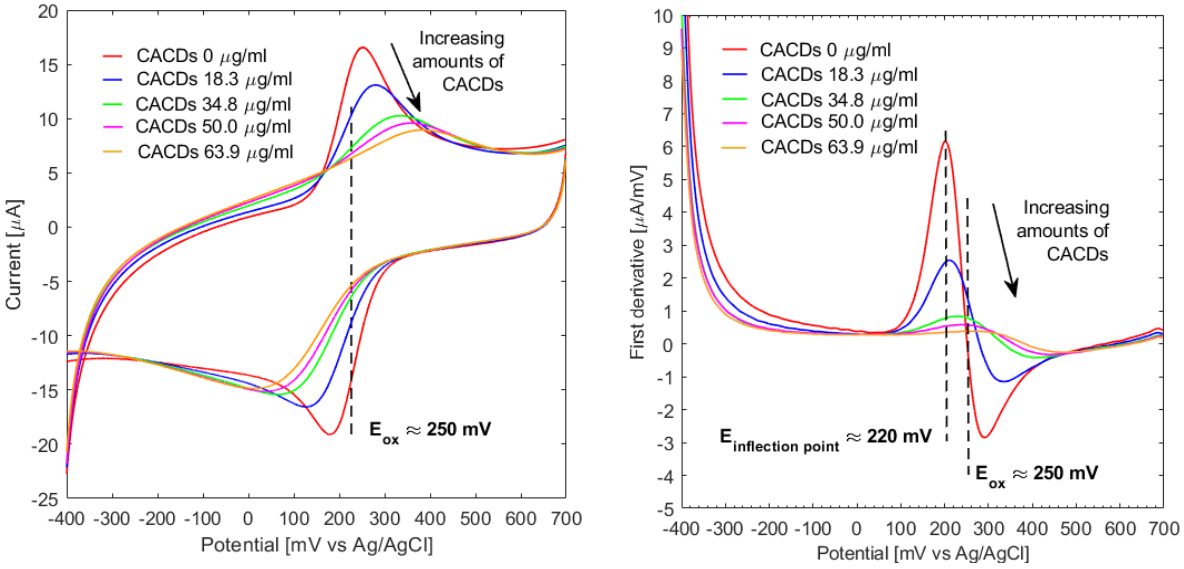

(a) (b)

Figure S21. (a) Cyclic voltametric profiles and (b) first derivative of voltametric profiles recorded utilizing 1 mM potassium ferricyanide (Aldrich) in 0.1 M KCl, obtained using 3mm GC Disk Electrode with the addition of increasing amounts of CA-CDs.
Scan rate: 100 mVs^{-1} (vs. Ag/AgCl).
E_{ox} - half-wave potentials for the oxidation of potassium ferricyanide ;
$E_{inflection\ point}$ - inflection point of the cyclic voltametric profiles, determined on the basis of the analysis of the first derivative.

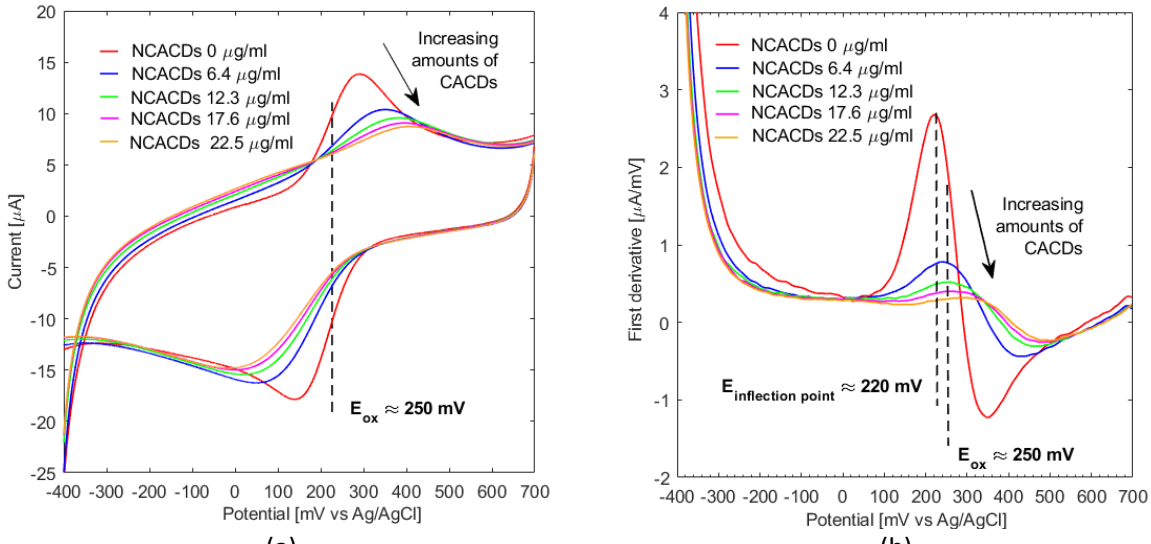

(a) (b)

Figure S22. (a) Cyclic voltametric profiles and (b) first derivative of voltametric profiles recorded utilizing 1 mM potassium ferricyanide (Aldrich) in 0.1 M KCl, obtained using 3mm GC Disk Electrode with the addition of increasing amounts of N-doped-C-ACDs.
Scan rate: 100 mVs^{-1} (vs. Ag/AgCl).
E_{ox} - half-wave potentials for the oxidation of potassium ferricyanide ;
$E_{inflection\ point}$ - inflection point of the cyclic voltametric profiles, determined on the basis of the analysis of the first derivative.

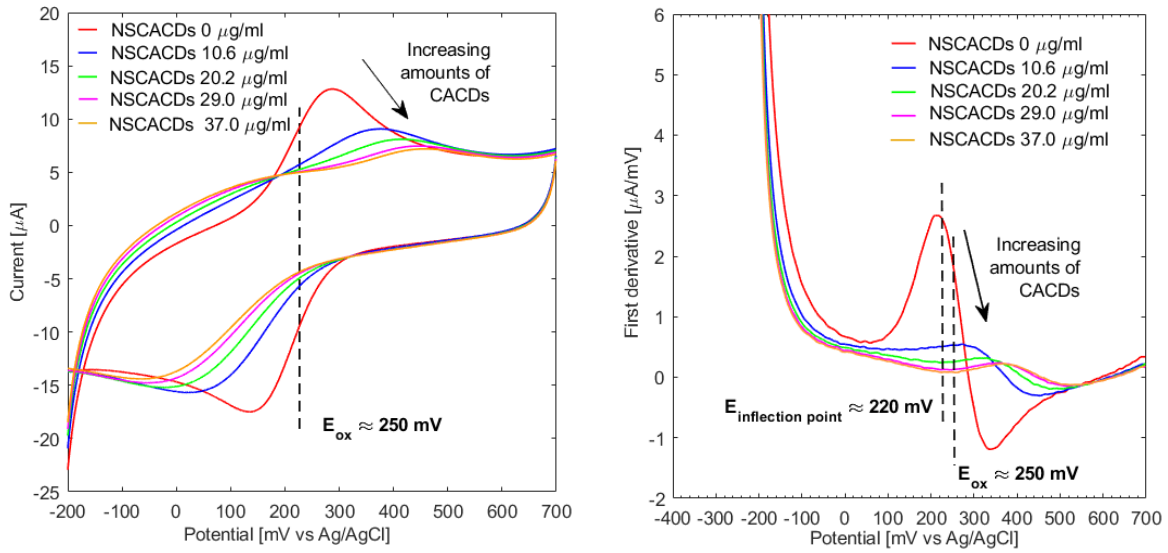

(a) (b)

Figure S23. (a) Cyclic voltametric profiles and (b) first derivative of voltametric profiles recorded utilizing 1 mM potassium ferricyanide (Aldrich) in 0.1 M KCl, obtained using 3mm GC Disk Electrode with the addition of increasing amounts of N,S-doped-CA-CDs.

Scan rate: 100 mVs^{-1} (vs. Ag/AgCl). E_{ox} - half-wave potentials for the oxidation of potassium ferricyanide ;

$E_{inflection\ point}$ - inflection point of the cyclic voltametric profiles, determined on the basis of the analysis of the first derivative.

3D printing of hydrogels in aqueous plotting media

Photo S1. 3D hydrogel inscription made by the free-radical photopolymerization of mixture HEA/water (1/1 wt.) in the presence of a two-component photoinitiating system based on CA-CDs (0.2 wt. %) and IOD (2 wt. %).

3D printing using cationic photocurable model resin

Photo S2. 3D inscription made by the cationic photopolymerization of vinyl monomer (TEGDVE)) in the presence of a two-component photoinitiating system based on CA-CDs (0.2 wt. %) and IOD (2 wt. %).

Mechanism proposal

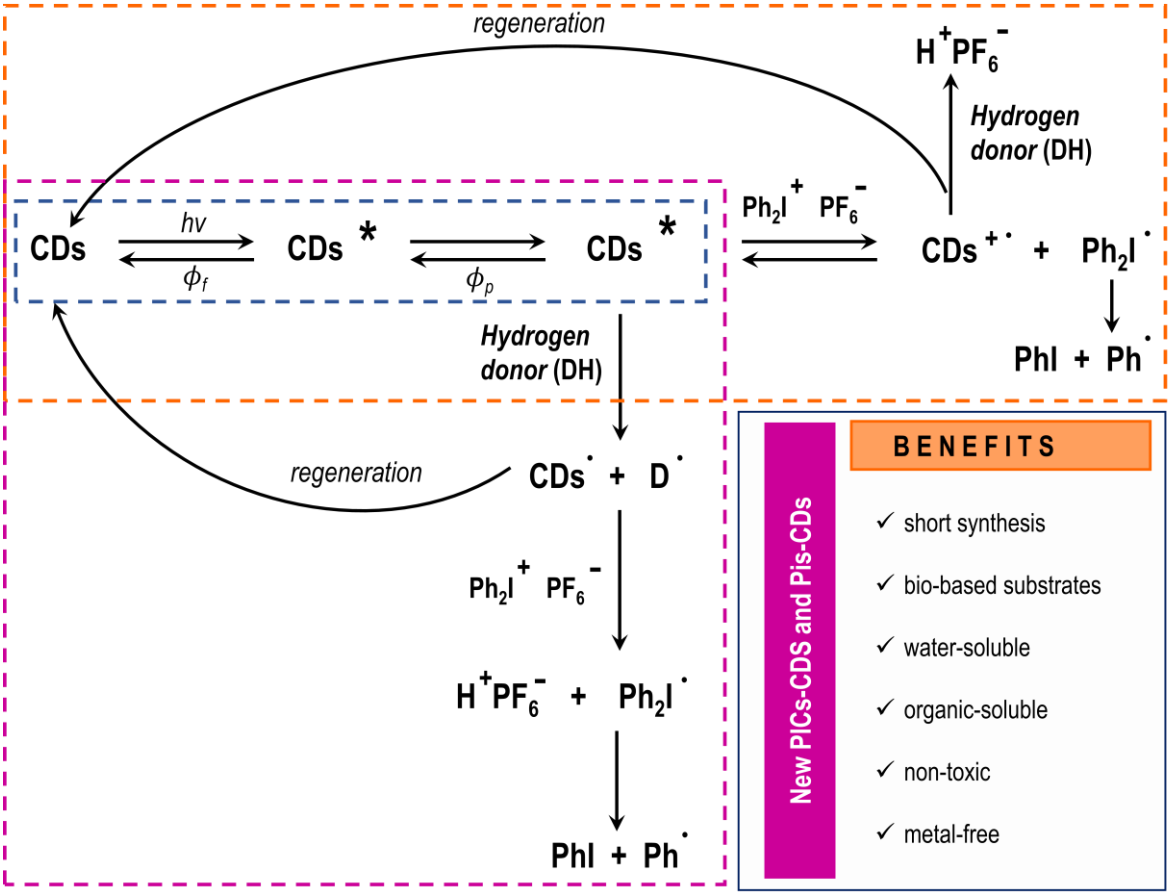

Figure S24. Scheme of the electron transfer mechanism proposal to generate the strong protonic acids.

SUPPORTING INFORMATION

Grafical abstract